Optimization of (Phenylmethylidene)-hydantoins as Prostate Cancer Migration Inhibitors: SAR-Directed Design, Synthesis, and Pharmacophore Modeling

by **Mudit Mudit**[1]) and **Khalid A. El Sayed***

Department of Basic Pharmaceutical Sciences, College of Pharmacy, University of Louisiana at Monroe, 1800 Bienville Drive, Monroe, Louisiana 71201, USA
(phone: +1 318 342 1725; fax: +1 318 342 1737; e-mail: elsayed@ulm.edu)

Prostate cancer is one of the most common cancer forms among males of Western countries. Natural products proved to be an unparalleled source of molecular diversity. The 4-(hydroxyphenylmethylidene)hydantoin (PMH; **1**), (5*Z*)-5-(4-hydroxybenzylidene)imidazolidine-2,4-dione, was isolated from the Red Sea sponge *Hemimycale arabica*, and recently showed junctional complexes stabilization, anti-invasive, and antimetastatic activities *in vitro* and *in vivo*. The related synthetic analogue, (5*Z*)-5-[4-(ethylsulfanyl)benzylidene]imidazolidine-2,4-dione (**2**), showed several-fold-improved *in vivo* antimetastatic properties against the highly invasive prostate cancer. To further optimize the activity of PMHs, various ligand-based strategies were used including the extension of the structure, structural simplification, linker extension, and computer-assisted CoMFA (Comparative Molecular Field Analysis) results. These strategies yielded thirty 2nd-generation PMHs, designed based on the 1st-generation PMHs, such as **1** and **2**. Wound-healing assay was selected to evaluate the *in vitro* anti-migratory potential of these new PMHs against the PC-3 cell line. Several active PMHs, including **10**, **13**, **24**, **29**, with nearly twelvefold enhancement of activity *vs.* **2**, were identified. Active compounds were then used to build a pharmacophore model using the SYBYL's DIStance COmparison technique (DISCOtech). Active PMHs were also screened for fragment-based drug likeness using the OSIRIS program, and an overall drug score was also calculated. Interestingly, the overall drug scores of **24** and **29** along with their anti-migratory activity were significantly greater than those of **1** and **2**. In conclusion, PMHs can be the appropriate scaffolds for the urgently needed drug candidates for the control of androgen independent prostate cancer.

1. Introduction. – Prostate cancer is the second leading cause of cancer-related death in men in the United States [1]. Surgery and radiation therapy constitute the currently available treatment options for localized and early-stage prostate cancer [2]. However, in patients with advanced metastatic disease, relapse of the condition is very common [2]. Treatment with androgen ablation therapy can cause the disease to become androgen-independent in nature, highly metastatic, chemoresistant, and life-threatening [3–5]. The poor clinical outcome with chemotherapeutic agents such as doxorubicin, mitoxantrone, and docetaxel in patients with hormone refractory prostate cancer urges the critical need for the discovery and development of alternative effective therapeutic agents.

[1]) Current Address: Department of Pharmaceutical Sciences, D'Youville College, School of Pharmacy, 320 Porter Avenue, Buffalo, New York 14201, USA.

© 2011 Verlag Helvetica Chimica Acta AG, Zürich

(Phenylmethylidene)-hydantoins (PMHs) are marine-derived compounds reported earlier from the Red Sea sponge *Hemimycale arabica* and showed good *in vitro* and *in vivo* activities against the highly metastatic androgen-independent human prostate cancer cells [6][7]. Several synthetic analogues related to the natural PMH **1** (*Table 1*)

Table 1. *Synthesized (Phenylmethylidene)hydantoin Analogues*

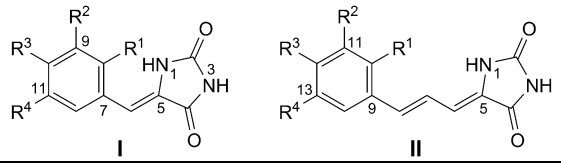

Compound	Type	Substituents				Reference
		R^1	R^2	R^3	R^4	
1	**I**	H	H	OH	H	[6]
2	**I**	H	H	EtS	H	[6]
3	**I**	H	H	HO–$(CH_2)_2$O	H	this work
4	**I**	H	H	$Me_2N(CH_2)_3O$	H	this work
5	**I**	H	H	^{t}BuO	H	this work
6	**I**	H	H	HC≡C	H	this work
7	**I**	H	H	$Me(CH_2)_6O$	H	this work
8	**I**	H	H	$Me(CH_2)_{15}O$	H	this work
9	**I**	H	H	1*H*-Tetrazol-5-yl	H	this work
10	**I**	Cl	H	NH_2	H	this work
11	**I**	H	NO_2	BuO	H	this work
12		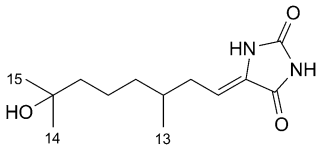				this work
13	**II**	H	H	Et_2N	H	this work
14	**II**	H	MeO	OH	H	this work
15	**I**	H	H	$MeSO_2$	H	[18]
16	**I**	H	H	HOOC	H	[19]
17	**I**	H	H	MeCONH	H	[a])
18	**I**	H	H	Me_2N	H	[20][21]
19	**I**	H	H	H_2C=$CHCH_2O$	H	[b])
20	**I**	H	H	$NC(CH_2)_2N(Me)$	H	[c])
21	**I**	H	H	$(HO–(CH_2)_2)_2N$	H	[22][23]
22	**I**	H	H	Bu_2N	H	[24]
23	**I**	H	H	$Me(CH_2)_5O$	H	[d])
24	**I**	H	H	(2,5-Dioxoimidazolidin-4-ylidene)methyl	H	[e])
25	**I**	H	OH	OH	H	[25]
26	**I**	H	MeO	OH	H	[20]
27	**I**	H	MeO	BuO	H	[f])
28	**I**	H	MeO	H	MeO	[26]
29	**I**	H	MeO	OH	MeO	[27][28]
30	**I**	H	MeO	OH	Cl	[29]

Table 1 (cont.)

Compound	Type	Substituents				Reference
		R^1	R^2	R^3	R^4	
31				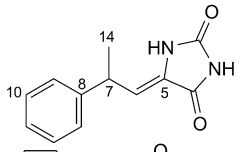		[g]
32				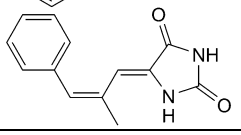		[30]

[a]) *CAS* registry No. 709023-48-3. [b]) *CAS* registry No. 432014-76-1. [c]) *CAS* registry No. 883101-39-1. [d]) *CAS* registry No. 894264-48-3. [e]) *CAS* registry No. 709620-57-5. [f]) *CAS* registry No. 462626-00-2. [g]) *CAS* registry No. 709644-05-3.

were also reported to show significant activities [6]. The natural PMH **1** and the synthetic (5*Z*)-5-[4-(ethylsulfanyl)benzylidene]imidazolidine-2,4-dione (**2**) showed potent anti-invasive and anti-migratory properties against PC-3M prostate cancer cells in various pharmacological assays including the spheroid disaggregation assay [6][7]. A 50 μM dose of PMH **1** significantly increased transepithelial resistance (TER) of diluent and CT- (calcitonin)-treated PC-3M cell cultures, suggesting that **1** promotes tight junctions (TJs) formation and completely reverses the action of CT on TER [6][7]. PMH **1** decreased baseline paracellular permeability and also abolished CT-induced increase in paracellular permeability of polarized PC-3M cell layers [6][7]. This effect further supported the fact that **1** promotes TJs formation. PMHs **1** and **2** showed prominent anti-invasive and anti-metastatic activities in an orthotopic xenograft model of PC-3M cells in nude mice [7]. They also decreased orthotopic tumor growth and inhibited the formation of tumor micrometastases in distant organs [7]. Further, PMH **2** also showed potent activity in LPB (long probasin promoter)-Tag (large T-antigen) transgenic mice model [7]. It remarkably reduced the growth of primary tumors and their metastasis in reproductive organs, decreased morbidity, and increased mice survival average. Thus, PMHs **1** and **2** were considered as novel leads appropriate for future optimizations as treatment for metastatic prostate cancers. The present study builds on the previous studies and targets further optimization of PMHs as a lead anti-migratory class to improve their potency level and to establish the structure–activity relationship by using diverse strategies.

2. Results and Discussion. – 2.1. *Design of New PMHs.* Previous CoMFA (Comparative Molecular Field Analysis) results generated by using a data set of 35 PMHs were used in part to design the 2nd-generation PMHs [6]. The results of the CoMFA are summarized as follows: *1*) Areas of high steric bulk tolerance (80% contribution) in *p*-position of the benzylidene group in PMH **2** were observed, and, therefore, the activity can be significantly enhanced by bulky groups in this position. *2*)

Bulky groups are sterically unfavorable in the *o*-positions of the benzylidene group; therefore, it should not possess any bulky groups. *3*) Electronegative (high electron density) groups in the *m*- and *p*-positions of the benzylidene group may show better activity (presence of substituted *O*, *N*, or *S* groups might increase the activity). *4*) Low-electron-density groups in *o*-position can improve the activity.

Several other strategies have also been used to design additional PMHs, for example extension of the structure, which involves the addition of extra-functional groups to the primary scaffold to probe for unused binding interactions with the target [8]. This can better target hydrophobic regions in the binding pocket of the receptor. Additional H-bonding interactions or ionic interactions can also be achieved by the substitution with appropriate functional groups [8–12]. The linking group or an extender sometimes play a significant activity role; especially if the terminal segments are known to improve the activity, extension of the linker might improve the interactions of these segments with their respective binding regions [8][13]. In homologation technique, chain length can be used for optimization. Extending the length of a saturated carbon side chain to five to nine atoms can sometimes increase the pharmacological activity, while further lengthening reduces the activity [14–16]. Pharmacophore modeling is a useful tool to find new pharmacophore moieties, when a structure–activity relationship (SAR) of a known compound is available. Pharmacophoric group determination can also be used in database searching to identify other novel classes sharing the common pharmacophoric features [17]. Pharmacophoric feature identification was illustrated successfully for hydroxamate inhibitors of the matrix metalloproteinases (MMPs) [17].

This study describes the use of ligand-based drug optimization techniques including CoMFA, dual substitutions at *m*- and *p*-positions, extension of the structure, linker extension, and homologation techniques. Pharmacophore modeling was then used for mapping essential pharmacophoric features needed for PMHs' activity and to validate the CoMFA results in terms of electrostatic requirements for the activity. Drug likeness was also evaluated for the active PMHs to assess their future potential as drug candidates.

2.2. *Chemistry.* Twelve new and eighteen known (**3**–**14** and **15**–**32**, resp.) PMHs were synthesized using the feasible regioselective and cost-effective base-catalyzed condensation reaction of hydantoin with various substituted aldehydes in the presence of 2-aminoethanol (*Table 1*, *Scheme*) [6].

Scheme. *General Synthesis of PMHs* **1**–**32** [6]

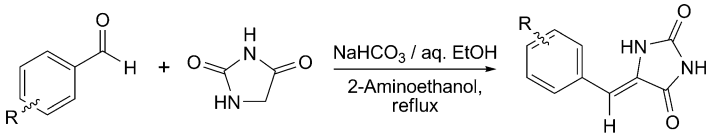

For example, the HR-EI-MS data of **3** showed a $[M-H]^+$ ion peak at *m*/*z* 247.0720, suggesting the molecular formula $C_{12}H_{12}N_2O_4$. The identity of **3** as (5*Z*)-5-[4-(2-hydroxyethoxy)benzylidene]imidazolidine-2,4-dione was established *via* analysis of its

^{1}H- and ^{13}C-NMR data. The *singlet* of the olefinic H–C(6)[2]) (δ(H) 6.39) showed HMBCs with the signals of aromatic C(8) and C(12) (δ(C) 131.7), and with the one of C(4) (δ(C) 166.2). Furthermore, the signal of H–C(6) showed HMBCs with the signals of quaternary C(5) and C(7) (δ(C) 125.9 and 126.6, resp.). In the COSY spectrum, the aromatic H-atom *doublet* at δ(H) 6.96 (H–C(9) and H–C(11)) correlated with the signal of H–C(8) and H–C(12) at δ(H) 7.58. The latter H-atoms also showed HMBCs with the signal of quaternary O-bearing C(10) (δ(C) 159.5) and C(7). The *triplet* CH_2(1′) (δ(H) 4.02) showed a HMBC with C(10) and COSY coupling with the neighboring *triplet* CH_2(2′) (δ(H) 3.72).

The HR-EI-MS data of **4** showed a $[M-H]^+$ ion peak at *m*/*z* 288.1353, which suggested a molecular formula of $C_{15}H_{19}N_3O_3$. The ^{1}H- and ^{13}C-NMR data of **4** confirmed the identity of the 3-(dimethylamino)propoxy moiety at C(10)[2]).

The HR-EI-MS data of **5** and **6** showed $[M-H]^+$ ion peaks at *m*/*z* 259.1084 and 211.0514, suggesting the molecular formulae $C_{14}H_{16}N_2O_3$ and $C_{12}H_8N_2O_2$, respectively. The ^{1}H- and ^{13}C-NMR data of **5** and **6** further confirmed their identity to be (5*Z*)-5-(4-*tert*-butoxybenzylidene)imidazolidine-2,4-dione and (5*Z*)-5-(4-ethynylbenzylidene)-imidazolidine-2,4-dione, respectively.

The HR-EI-MS data of **7** and **8** showed $[M-H]^+$ ion peaks at *m*/*z* 301.1550 and 427.2965, consistent with the molecular formulae $C_{17}H_{22}N_2O_3$ and $C_{26}H_{40}N_2O_3$, respectively. Their ^{1}H- and ^{13}C-NMR data confirmed their identity as (5*Z*)-5-[4-(heptyloxy)benzylidene]imidazolidine-2,4-dione and (5*Z*)-5-[4-(hexadecyloxy)benzyl-idene]imidazolidine-2,4-dione, respectively.

The ^{1}H- and ^{13}C-NMR data of **9**–**11**, along with their HR-EI-MS, suggested the proposed structures.

Analysis of various spectral data indicated that **12** is (5*Z*)-5-(7-hydroxy-3,7-dimethyloctylidene)imidazolidine-2,4-dione. The olefinic H–C(6)[2]) (δ(H) 5.50) showed HMBCs with the amide CO of the hydantoin ring (δ(C) 164.9) and the CH group C(8) (δ(C) 33.2). A COSY experiment connected the segment H–C(6)–CH_2(11)/Me(13). The *doublet* of Me(13) (δ(H) 0.86) showed HMBCs with C(7) (δ(C) 33.8), C(9) (δ(C) 37.3), and with C(8). Similarly, the Me *singlet*s Me(14) and Me(15) showed HMBCs with C(12) (δ(C) 69.3) and C(11) (δ(C) 44.4), confirming the structure of the side chain.

The HR-MS, ^{1}H- and ^{13}C-NMR data identified **13** as (5*Z*)-5-{(2*E*)-3-[4-(diethyl-amino)phenyl]prop-2-en-1-ylidene}imidazolidine-2,4-dione. The *doublet* for the olefinic H–C(6)[2]) appeared at δ(H) 6.22, and showed HMBCs with the signal for a CO group (δ(C) 165.2) and the one for the olefinic CH group C(8) (δ(C) 138.6). A COSY experiment connected the segment H–C(6)–H–C(8). The signal for H–C(10) and H–C(14) (δ(H) 7.31) showed HMBCs with those of C(8) and N-bearing quaternary C(12) (δ(C) 148.3). Similarly, the *doublet* for H–C(11) and H–C(13) (δ(H) 6.66) showed a HMBC with the signal for quaternary aromatic C(9) (δ(C) 124.1). The *triplet* for Me(2′) (δ(H) 1.10) showed COSY coupling with the *quartet* for CH_2(1′) (δ(H) 3.37). This *quartet* also showed a HMBC with C(12). Compound **14** showed similar NMR data to that of **13** with different R^2 and R^3 substitution patterns.

---

[2]) Arbitrary numbering; see *Table 1*. For systematic names, see *Exper. Part.*

2.3. *Biological Evaluation and SAR Studies.* During the process of metastasis, the primary tumor tends to spread from its primary site to its preferable secondary tissues or organs [31][32]. In this multistep process, cell migration comprises a major contributing factor. Any failure in this multistep process, including the cell migration, could block the entire metastatic process. Wound-healing assay is a classical and commonly used method for studying cell migration [33]. A scratched cell monolayer heals the wound in a characteristic manner; therefore, this assay is widely used to study cell migration rates, cell polarization, and matrix remodeling studies [34–36]. The wound-healing assay can be used for the validation of small molecule leads that affect cell migration and for detailed cell biological studies [37–40]. This assay proved useful as a proxy for metastasis, angiogenesis, and other pathophysiological and physiological processes. Therefore, the wound-healing assay is used in this study to identify and rank the anti-migratory potential of synthesized PMHs [41–46].

In this study, 30 PMHs were designed and synthesized to identify an optimized lead for the control of androgen independent prostate cancer. The design of these compounds was based in part on the earlier CoMFA results [6]. Different tactics were utilized to modify PMHs and optimize their anti-migratory activity. The anti-migratory activities of PMHs **3**–**32** using the wound-healing assay are shown in *Table 2*. These compounds did not show any cytotoxicity at the tested doses, as evidenced by no significant affect on cell viability in MTT assay. The IC_{50} values were calculated for those compounds more active than PMH **2** (*Table 2*). *Figs. 1* and *2* show the dose–response effects for the PMHs more active than **2**.

Type **I** compounds contain electronegative groups in the *m*- and *p*-positions. In order to expand the series, sterically demanding substitutents were introduced in these positions. Additionally, compounds with substitutents both in *m*- and *p*-position were prepared, **11**, **25**–**27**, **29**, **30**, as well as a compound substituted in both *m*-positions, **28**.

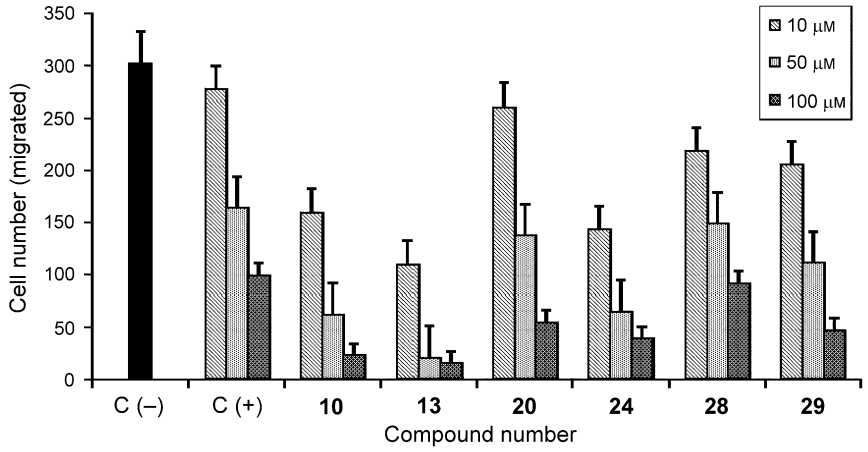

Fig. 1. *Anti-migratory activity of* **10**, **13**, **20**, **24**, **28**, *and* **29** *on highly metastatic PC-3 prostate adenocarcinoma cells in the wound-healing assay.* Active compounds are shown with respect to PMH **2**. PMH **2** is taken as the positive control, C (+). Vehicle control is represented by C (–). Column height indicates the mean value for three replicates in each treatment group.

Table 2. *Anti-migratory Activity of PMHs* **1**–**32** *against PC-3 Cells using Wound-Healing Assay*

Compound	Anti-migratory activity	
	% Migration (IC_{50} [μM][a])	Activity rank[b])
1	74.0 (139.2)	–
2	60.8 (51.4)	–
3	95.9	1
4	94.3	1
5	79.0	1
6	100.0	1
7	97.2	1
8	99.4	1
9	89.5	1
10	33.2 (9.5)	3
11	68.7	2
12	100.1	1
13	15.9 (4.2)	3
14	65.8	2
15	95.1	1
16	76.7	1
17	87.1	1
18	69.2	2
19	94.0	1
20	47.8 (50.1)	3
21	76.8	1
22	100.3	1
23	96.6	1
24	28.4 (5.7)	3
25	72.7	2
26	65.0	2
27	99.7	1
28	54.5 (50.1)	3
29	43.6 (21.6)	3
30	67.2	2
31	99.3	1
32	73.2	2

[a]) IC_{50} values were calculated for compounds with activity level better than **2**. [b]) Anti-migratory activity ranking: rank-1: Activity $\leq$ compared to the activity of **1**. rank-2: Activity $>$ activity of **1** and $<$ than the activity of **2**. rank-3: Activity $>$ than the activity of **2**.

The active functional groups reported earlier were used. Among these, **11**, **25**, **26**, and **30** were more active than PMH **1**, while **28** and **29** were even more active than the most active PMH **2** earlier reported. In **7**, **8**, and **23**, C(10) was substituted with a long saturated carbon side chain attached to an O-atom, but this homologation did not improve the activity. These results were consistent with earlier results that showed that increasing the number of saturated C-atoms attached to an O-atom even to two or four C-atoms can reduce the activity [6]. Similarly, the saturated carbon side chain attached to N-atoms was modified to one- and four-C-atom length in the case of **18** and **22**, respectively. In an earlier report, enhanced activity of PMHs with two C-atoms in the

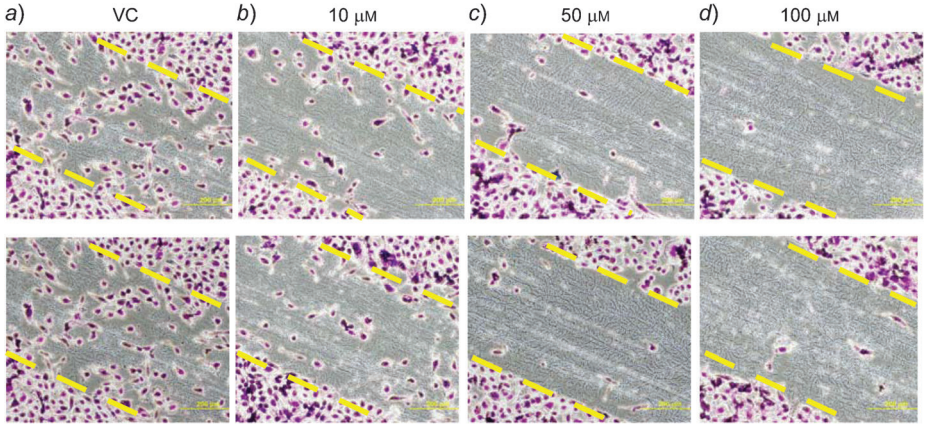

Fig. 2. *Wound-healing assay using PC-3 cells after 24 h of incubation with various doses of* **24** (upper row) *and* **29** (lower row) versus *vehicle control* (VC). $X = 100$.

saturated side chain attached to an N-atom at C(10) was described [6]. The lack of activity of **22** suggests the complete loss of activity with a side chain with four C-atoms. Type **I** PMHs retained the PMH moiety. An overall extension of the structure was attempted with substituents to possibly increase the extent of binding interactions with the binding regions at the target receptor pocket.

The necessity of a C(10) free OH group for the activity was investigated. Interestingly, a significant increase in activity was observed for **10**, where the OH group was replaced by an NH_2 group at this position, and an additional Cl substituted at C(8), which counteracted the difference of lipophilicity between the OH and NH_2 groups (*Table 2*). In an earlier report [6], a PMH with a Cl–C(8) group had a similar activity as PMH **1** with a HO–C(10) group. The Cl–C(8) moiety was presumed to sufficiently increase the lipophilicity, without significantly compromising the steric effects at this position due to its smaller atomic radius. Activity improvement of **10** can also be explained by the presence of an H-bond acceptor (HBA) N-atom in *p*-position (C(10), as also evidenced by pharmacophore modeling for activity increment). It can also be interpreted that H-bond donor (HBD) groups are not crucial at this position, as concluded by the increased activity of **10** *versus* **1** (the NH_2 group has lower H-bond donating ability than the OH group). The same conclusion can further be supported by the improved activities of compounds with EtS, Me_2N, and Et_2N groups, which have no HBD groups at the *p*-position (C(10)). This was also consistent with the pharmacophore modeling results, which suggested the necessity of the presence of HBA pharmacophore at C(10) for the activity.

In **31** and **32**, the connection of the two rings contains a chain of two and three C-atoms, respectively, with a Me substituent. While **31** was completely inactive, **32** was comparable to **1** in activity. Therefore, type **II** molecules **13** and **14** were synthesized with a three-C-atom linker in conjunction with earlier active groups in the *m*- and *p*-positions [6]. Compound **13** showed the most promising anti-migratory activity, which highlights the potential of 5-[3-phenylprop-2-en-1-ylidene]imidazolidine-2,4-diones as

a novel anti-migratory class. The justification of activity enhancement of **13** might be attributed to the presence of the three-C-atom linker in addition to the terminal active Et_2N group.

In **12**, an aliphatic side chain replaced the Ph ring, while the OH group was maintained in the terminal part. The complete loss of anti-migratory activity of **12** in highly metastatic PC-3 prostate cells further suggest that the Ph moiety plays a crucial role for this activity.

2.4. *Pharmacophore Modeling.* DIStance COmparison technique (DISCOtech) based on 3D pharmacophore mapping methodology was used to build the pharmacophore for the five active analogues **10**, **20**, **24**, **28**, and **29** [47][48]. *DISCOtech*™ is a well-established module to design pharmacophoric maps and is based on the assumption that a given set of active molecules, which are related by their pharmacological activities, may possess consensus features in structural distance space [49][50]. The identification of common pharmacophoric model features in the molecule can be accomplished by using SYBYL's *DISCOtech*™. The pharmacophoric elements taken to construct this model include H-bond donor (HBD) atoms, H-bond acceptor (HBA) atoms, and hydrophobic centers. *DISCOtech*™ can be efficiently used with as low as three to five active compounds to generate a pharmacophore model [49–52].

In the present study, 100 conformers were generated for each compound with the individual pair-wise tolerance value ranging from 0.5 to 2.0. A stochastic search method was used to create these conformers. Ten *DISCOtech* pharmacophoric runs (*Table 3*) were performed by varying the tolerance and range of required features. The pair-wise tolerance value was optimized to accommodate the range of pharmacophoric features with the highest score. Highest scores for top 5 pharmacophoric models in any individual *DISCOtech* run are listed in *Table 3*. The final *DISCOtech* pharmacophore model with the highest score, reflecting a maximum structural overlap, and a maximum number of pharmacophoric features was proposed (*Fig. 3*). This model has three HBA ligands (AL-1 to AL-3), two HBD ligands (DL-1 and DL-2), and two hydrophobic centers (HY-1 and HY-2). It is worth noting that pharmacophore modeling of PMHs was reported earlier for the search for glycogen synthase kinase-3β inhibitors [53]. In

Table 3. *Number of Pharmacophoric Features and Top 5 High Score Ranges for Each of the DISCO Pharmacophoric Run*

Run Name	Feature Range	Tolerance	Models	Total Features	Top 5 Score Range	Features in Top Scored Model
DISC-1 (a)	3–7	0.5	50	5	2.2874–2.2877	2DL, 2AL, 1 HY
DISC-1 (b)	3–7	1.0	100	5	2.7901–2.7902	2DL, 1AL, 2 HY
DISC-1 (c)	3–7	1.5	52	6	2.8406–3.1067	2DL, 2AL, 2 HY
DISC-1 (d)	3–7	1.85	57	7	3.1137–4.1223	2DL, 2AL, 3 HY
DISC-1 (e)	3–7	2.0	153	7	3.6326–4.1324	2DL, 2AL, 3 HY
DISC-2 (a)	7–15	0.5	49	6	4.3496–4.3497	2DL, 2AL, 1 HY
DISC-2 (b)	7–15	1.0	49	6	4.3496–4.3497	2DL, 2AL, 1 HY
DISC-2 (c)	7–15	1.5	49	6	3.3498–3.3499	2DL, 2AL, 1 HY
DISC-2 (d)	**7–15**	**1.85**	**52**	**7**	**4.0532–4.5373**	**2DL, 3AL, 2 HY**
DISC-2 (e)	7–15	2.0	57	7	4.1238–4.5095	2DL, 3AL, 2 HY

the present pharmacophore modeling study, the tolerance parameters were set more relaxed (1.0–1.85) to accommodate maximum relevant pharmacophoric features, since the exact molecular target is not known. Distance relationships between various pharmacophoric features are denoted in *Fig. 4*.

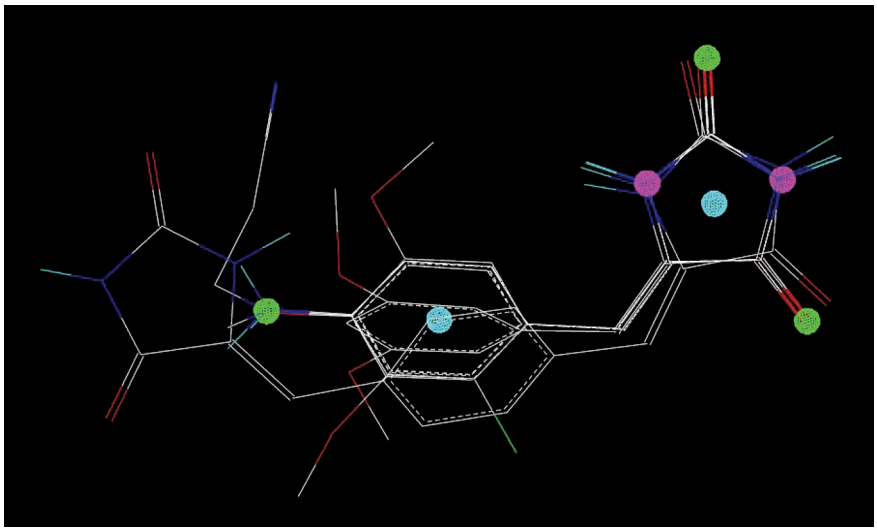

Fig. 3. *Pharmacophoric features generated by using overlaid active PMHs* **10**, **20**, **24**, **28**, *and* **29**. Color codes: blue, hydrophobic center; green, HBA site; pink, HBD site.

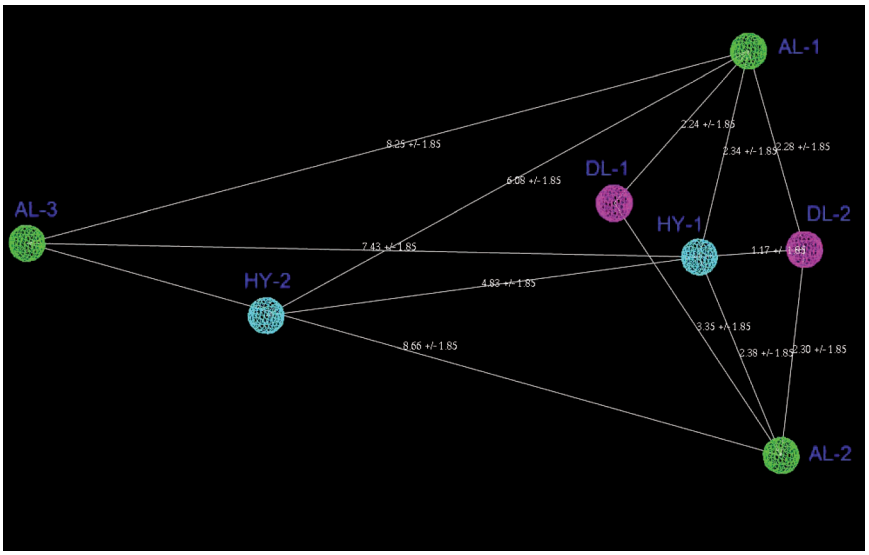

Fig. 4. *Pharmacophoric features of active PMHs and their distance relationship generated by* DISCOtech™ *module.* AL-1/AL-2/AL-3, H-bond acceptor ligands; DL-1/DL-2, H-bond donor ligands; HY-1/HY-2, hydrophobic centers.

2.5. In silico *ADMET Screening*. Drug-likeness of a compound can be assessed by many approaches based on topological descriptors, fingerprints of molecular drug likeness (MDL) structure keys, or other common properties such as clog*P* and molecular weights [54]. Approaches for early ADMETox profiling, and new understandings with respect to molecular pharmacodynamics, have been rapidly evolving, providing guidance and enabling early conclusions that were not available several years ago, when several clinical trials failed due to poor ADMETox characters of drug candidates. In the present study, the OSIRIS program was used to explicit these properties. OSIRIS involves the database of traded drugs and supposedly non-drug-like *Fluka* compounds to assess the occurrence frequency of each fragment in the individual structure. Fragment-based drug-likeness of the four most active PMHs were evaluated and compared with the reported anti-metastatic PMHs **1** and **2** (*Fig. 5*). Interestingly, the potential drug-likeness value of **29** was significantly higher than PMHs **1** and **2**, while **13** showed a negative value with possible induction of toxicity. Furthermore, **24** also showed significant drug-likeness.

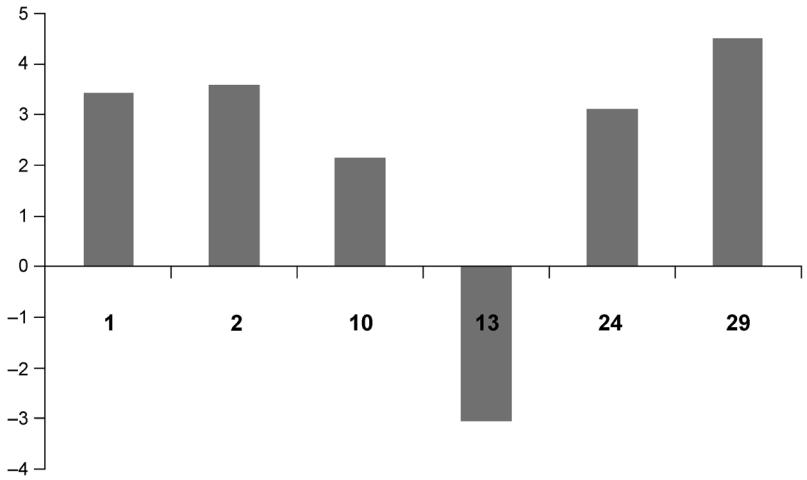

Fig. 5. *Drug-likeness of active PMHs* **10**, **13**, **24**, *and* **29** *compared to PMHs* **1** *and* **2**

In addition, the overall drug score was evaluated, which is a combined outcome of drug-likeness, molecular weight, log*S*, clog*P*, and toxicity risks, encompassing mutagenicity, tumorigenicity, irritating, and reproductive effects [55]. Drug score is important in predicting a compound's potential to meet the criteria's of a possible drug candidate [55]. *Fig. 6* shows comparable drug scores for the PMHs **24** and **29**, which were significantly better than the reported PMHs **1** and **2**. Interestingly, **24** was never correlated with any biological activity, while a patent was awarded on anti-allergic and anti-inflammatory activities of related structures including **29**, which revealed that it was devoid of both activities [27][28]. The structural features of PMHs **24** and **29** are commonly present in the traded drugs, and therefore they might qualify as potential drug candidates for the control and prevention of metastatic androgen independent prostate cancer.

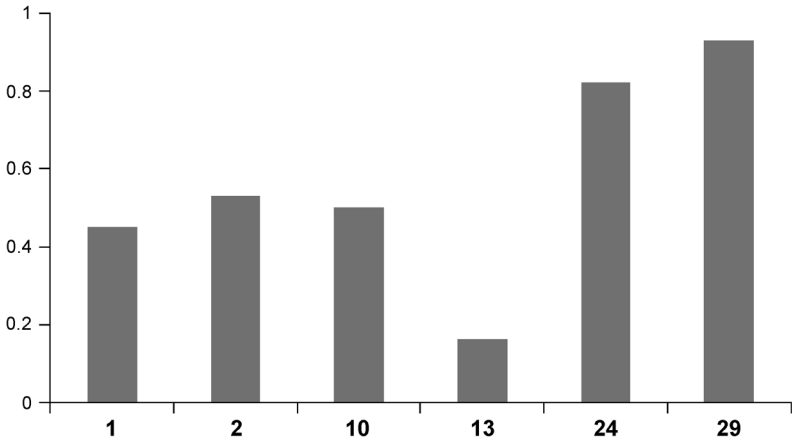

Fig. 6. *Overall drug score values of active PMHs* **10**, **13**, **24**, *and* **29** *compared to those of PMHs* **1** *and* **2**

3. Summary of SAR and Conclusions. – The SAR studies suggest the following: *1*. R^3 Substitution is critical for the anti-migratory activity based on the activity of **28** *versus* **29**. A HBA atom is required at this position as evidenced by the pharmacophore modeling. *2*. If O is the HBA atom, the R^3 position can not hold alkoxy substituents with more than one C-atom, while one or two C-atoms attached to an N- or S-containing substituent seem reasonable for the activity. *3*. An electronegative R^3 group contributes more by behaving as a HBA moiety as opposed to HBD for the activity. *4*. Combined electronegative groups at R^2, R^3, and R^4 positions seem to have an additive effect for the activity as seen in **28** and **29**. *5*. A linker containing a three-C-atoms chain, with (*E*)-oriented C=C bond geometry, between the hydantoin and the Ph ring proved superior *vs.* a linker containing only one or two C-atoms, as suggested by the active phenylallylidene hydantoin **13**. *6*. The presence of the Ph ring is crucial for the activity as evidenced by the lack of activity of **12**.

PMHs proved effective in inhibiting cell migration, and therefore we can suggest that they interfere with metastasis. Hence, PMHs could be valuable leads not only to limit the spread of existing tumors, but also can control new tumor formation and micrometastases. Therefore, PMHs can be used for chemoprevention in addition to possible concomitant use with chemotherapeutic agents for the control of metastatic prostate cancer.

This study was supported in part by the *Louisiana Biomedical Research Network*.

Experimental Part

General Experimental Procedures. TLC Analyses: precoated silica gel *60* F_{254} 500 μm TLC plates (*EMD Chemicals*), using MeOH/$CHCl_3$ 1:9 as a developing eluent. Column chromatography (CC): silica gel *60* (SiO_2; particle size 63–200 μm; *Natland International*). Optical rotation: *Rudolph Research Analytical Autopol III* polarimeter. IR Spectra: *Varian 800 FT-IR* spectrophotometer. ^{1}H- and ^{13}C-NMR spectra: in (D_6)DMSO; with TMS as an internal standard; *JEOL Eclipse-400* NMR spectrometer

operating at 400 MHz for ^{1}H and 100 MHz for ^{13}C. HR-EI-MS: conducted at Louisiana State University on a *6200-TOF LCMS* (*Agilent*) instrument equipped with a multimode source (mixed source that can ionize the samples alternatively by ESI and APCI).

Preparation of PMHs. A two-neck round bottom flask was used to dissolve hydantoin (1.0 g) in 10 ml H_2O by heating at 70° in an oil bath with continuous stirring [6]. A sat. soln. of $NaHCO_3$ was used to maintain the pH at 7.0 [6]. 2-Aminoethanol (0.9 ml) was then added and the temp. was raised to 90° [6]. An equimolar quantity of substituted benzaldehyde dissolved in 10 ml of EtOH was then added dropwise [6]. The mixture was kept under reflux for 10 h. The reaction was monitored by TLC every hour and the endpoint of the reaction was visualized by the formation of a precipitate. The mixture was then cooled to 4°, and the precipitate was filtered, washed with EtOH/H_2O 1:5, and then recrystallized from EtOH. Yields of the product ranged from 60–90%, based on the nature of individual aldehyde.

(5Z)-5-[4-(2-Hydroxyethoxy)benzylidene]imidazolidine-2,4-dione (**3**). White amorphous solid. IR ($CHCl_3$): 3274, 1734, 1717, 1653. ^{1}H-NMR: 7.58 (*d*, *J* = 8.4, H–C(8), H–C(12)^2)); 6.96 (*d*, *J* = 8.8, H–C(9), H–C(11)); 6.39 (*s*, H–C(6)); 4.02 (*t*, *J* = 4.8, CH_2(1′)); 3.72 (*t*, *J* = 4.8, CH_2(2′)). ^{13}C-NMR: 166.2 (*s*, C(4)); 159.5 (*s*, C(10)); 156.2 (*s*, C(2)); 131.7 (*d*, C(8), C(12)); 126.6 (*s*, C(7)); 125.9 (*s*, C(5)); 115.4 (*d*, C(9), C(11)); 109.3 (*d*, C(6)); 70.2 (*t*, C(1′)); 60.1 (*t*, C(2′)). HR-EI-MS: 247.0720 ($[M-H]^+$, $C_{12}H_{11}N_2O_4^+$; calc. 247.0719).

(5Z)-5-[4-[3-(Dimethylamino)propoxy]benzylidene]imidazolidine-2,4-dione (**4**). White amorphous solid. IR ($CHCl_3$): 3159, 1716, 1670, 1654. ^{1}H-NMR: 7.57 (*d*, *J* = 8.8); 6.94 (*d*, *J* = 8.8); 6.38 (*s*); 4.03 (*t*, *J* = 6.6); 2.34 (*t*, *J* = 7.0); 2.14 (*s*); 1.84 (*tt*, *J* = 6.6). ^{13}C-NMR: 166.2 (*s*); 159.4 (*s*); 156.3 (*s*); 131.7 (*d*); 126.6 (*s*); 125.9 (*s*); 115.3 (*d*); 109.2 (*d*); 66.5 (*t*); 56.2 (*t*); 45.8 (*q*); 27.4 (*t*). HR-EI-MS: 288.1353 ($[M-H]^+$, $C_{15}H_{18}N_3O_3^+$; calc. 288.1348).

*(5Z)-5-(4-*tert*-Butoxybenzylidene)imidazolidine-2,4-dione* (**5**). Yellow amorphous solid. IR ($CHCl_3$): 3209, 1748, 1725. ^{1}H-NMR: 7.55 (*d*, *J* = 8.8); 6.98 (*d*, *J* = 8.4); 6.40 (*s*); 1.32 (*s*). ^{13}C-NMR: 166.2 (*s*); 156.2 (*s*); 156.1 (*s*); 131.0 (*d*); 128.2 (*s*); 127.4 (*s*); 124.0 (*d*); 108.9 (*d*); 79.2 (*s*); 29.1 (*q*). HR-EI-MS: 259.1084 ($[M-H]^+$, $C_{14}H_{15}N_2O_3^+$; calc. 259.1083).

(5Z)-5-(4-Ethynylbenzylidene)imidazolidine-2,4-dione (**6**). Yellow amorphous solid. IR ($CHCl_3$): 1734, 1717, 1653. ^{1}H-NMR: 7.63 (*d*, *J* = 8.4); 7.50 (*d*, *J* = 8.4); 6.41 (*s*); 4.32 (*s*). ^{13}C-NMR: 165.8 (*s*); 156.1 (*s*); 134.1 (*s*); 132.5 (*d*); 130.0 (*d*); 129.1 (*s*); 121.8 (*s*); 107.7 (*d*); 83.9 (*s*); 82.8 (*d*). HR-EI-MS: 211.0514 ($[M-H]^+$, $C_{12}H_7N_2O_2^+$; calc. 211.0508).

(5Z)-5-[4-(Heptyloxy)benzylidene]imidazolidine-2,4-dione (**7**). White amorphous solid. IR ($CHCl_3$): 3429, 2928, 2856, 1747, 1734. ^{1}H-NMR: 7.57 (*d*, *J* = 8.8); 6.94 (*d*, *J* = 8.8); 6.37 (*s*); 3.99 (*t*, *J* = 6.2); 1.71 (*tt*, *J* = 6.6); 1.40 (*tt*, *J* = 6.2); 1.27–1.29 (*m*); 0.87 (*t*, *J* = 6.6). ^{13}C-NMR: 166.4 (*s*); 159.4 (*s*); 157.4 (*s*); 131.6 (*d*); 125.9 (*s*); 124.2 (*s*); 115.3 (*d*); 109.1 (*d*); 68.1 (*t*); 31.8 (*t*); 29.2 (*t*); 29.0 (*t*); 26.0 (*t*); 22.6 (*t*); 14.5 (*q*). HR-EI-MS: 301.1550 ($[M-H]^+$, $C_{17}H_{21}N_2O_3^+$; calc. 301.1552).

(5Z)-5-[4-(Hexadecyloxy)benzylidene]imidazolidine-2,4-dione (**8**). White amorphous solid. IR ($CHCl_3$): 2926, 2852, 1718, 1661. ^{1}H-NMR: 7.34 (*d*, *J* = 8.8); 6.91 (*d*, *J* = 8.4); 6.60 (*s*); 3.96 (*t*, *J* = 6.6); 1.76 (*tt*, *J* = 7.0); 1.42 (*tt*, *J* = 7.0); 1.20–1.24 (*m*); 0.84 (*t*, *J* = 6.6). ^{13}C-NMR: 163.5 (*s*); 160.0 (*s*); 155.9 (*s*); 130.7 (*d*); 125.3 (*s*); 115.2 (*d*); 112.2 (*d*); 68.3 (*t*); 32.0 (*t*); 29.8 (*t*); 29.7 (*t*); 29.6 (*t*); 29.4 (*t*); 29.2 (*t*); 26.1 (*t*); 22.8 (*t*); 14.2 (*q*). HR-EI-MS: 427.2965 ($[M-H]^+$; $C_{26}H_{39}N_2O_3^+$; calc. 427.2961).

*(5Z)-5-[4-(1*H*-Tetrazol-5-yl)benzylidene]imidazolidine-2,4-dione* (**9**). Yellow amorphous solid. IR ($CHCl_3$): 1716, 1699, 1653. ^{1}H-NMR: 8.00 (*d*, *J* = 8.0); 7.65 (*d*, *J* = 8.4); 6.43 (*s*). ^{13}C-NMR: 166.2 (*s*); 160.7 (*s*); 156.3 (*s*); 132.8 (*s*); 132.1 (*s*); 130.2 (*d*); 128.0 (*s*); 126.6 (*d*); 109.1 (*d*). HR-EI-MS: 255.0634 ($[M-H]^+$; $C_{11}H_7N_6O_2^+$; calc. 255.0630).

(5Z)-5-(4-Amino-2-chlorobenzylidene)imidazolidine-2,4-dione (**10**). Yellow amorphous solid. IR ($CHCl_3$): 3420, 3338, 1733, 1717, 1654. ^{1}H-NMR: 7.47 (*d*, *J* = 8.8); 6.68 (*d*, *J* = 2.6); 6.55 (*s*); 6.53 (*s*, *J* = 2.2). ^{13}C-NMR: 166.1 (*s*); 156.1 (*s*); 151.2 (*s*); 135.2 (*s*); 131.2 (*d*); 126.0 (*s*); 117.6 (*s*); 114.1 (*d*); 113.4 (*d*); 105.5 (*d*). HR-EI-MS: 236.0227 ($[M-H]^+$; $C_{10}H_7ClN_3O_2^+$; calc. 236.0227).

(5Z)-5-(4-Butoxy-3-nitrobenzylidene)imidazolidine-2,4-dione (**11**). Yellow amorphous solid. IR ($CHCl_3$): 1750, 1716, 1654. ^{1}H-NMR: 8.08 (*d*, *J* = 2.2); 7.82 (*dd*, *J* = 2.2, 8.8); 7.40 (*d*, *J* = 8.8); 6.44 (*s*); 4.19 (*t*, *J* = 6.2); 1.70 (*tt*, *J* = 6.6); 1.42 (*qt*, *J* = 7.3); 0.92 (*t*, *J* = 7.3). ^{13}C-NMR: 165.8 (*s*); 156.2 (*s*); 151.1 (*s*); 140.5 (*s*); 135.5 (*d*); 128.6 (*s*); 126.0 (*s*); 125.3 (*d*); 115.7 (*d*); 106.5 (*d*); 69.6 (*t*); 31.0 (*t*); 19.1 (*t*); 14.1 (*q*). HR-EI-MS: 304.0939 ($[M-H]^+$; $C_{14}H_{14}N_3O_5^+$; calc. 304.0933).

(5Z)-5-(7-Hydroxy-3,7-dimethyloctylidene)imidazolidine-2,4-dione (**12**). White amorphous solid. IR ($CHCl_3$): 3365, 2963, 2938, 1748, 1718, 1684. ^{1}H-NMR: 5.50 (*dd*, *J* = 8.4, 8.1); 2.12–2.14 (*m*); 2.01–2.05 (*m*); 1.56–1.58 (*m*); 1.27–1.29 (*m*); 1.22–1.24 (*m*); 1.05 (*s*); 0.86 (*d*, *J* = 6.6). ^{13}C-NMR: 164.9 (*s*); 155.5 (*s*); 131.7 (*s*); 111.1 (*d*); 69.3 (*s*); 44.4 (*t*); 37.3 (*t*); 33.8 (*t*); 33.2 (*d*); 29.8 (*q*); 21.9 (*t*); 19.9 (*q*). HR-EI-MS: 253.1556 ($[M-H]^+$; $C_{13}H_{21}N_2O_3^+$; calc. 253.1552).

(5Z)-5-{(2E)-3-[4-(Diethylamino)phenyl]prop-2-en-1-ylidene}imidazolidine-2,4-dione (**13**). Red amorphous solid. IR ($CHCl_3$): 1771, 1734, 1589. ^{1}H-NMR: 7.31 (*d*, *J* = 8.4); 6.97 (*dd*, *J* = 12.1, 14.6); 6.79 (*d*, *J* = 15.4); 6.66 (*d*, *J* = 8.4); 6.22 (*d*, *J* = 11.7); 3.37 (*q*, *J* = 7.0); 1.10 (*t*, *J* = 7.0). ^{13}C-NMR: 165.2 (*s*); 154.9 (*s*); 148.3 (*s*); 138.6 (*d*); 129.0 (*d*); 127.5 (*s*); 124.1 (*s*); 117.5 (*d*); 111.9 (*d*); 111.4 (*d*); 40.5 (*t*); 13.1 (*q*). HR-EI-MS: 284.1404 ($[M-H]^+$; $C_{16}H_{18}N_3O_2^+$; calc. 284.1399).

(5Z)-5-[(2E)-3-(4-Hydroxy-3-methoxyphenyl)prop-2-en-1-ylidene]imidazolidine-2,4-dione (**14**). Orange amorphous solid. IR ($CHCl_3$): 3446, 3153, 1716, 1699, 1653. ^{1}H-NMR: 7.12 (*d*, *J* = 1.8); 7.07 (*dd*, *J* = 12.1, 15.4); 6.91 (*dd*, *J* = 1.5, 8.2); 6.82 (*d*, *J* = 15.4); 6.77 (*d*, *J* = 8.1); 6.23 (*d*, *J* = 11.7); 3.90 (*s*). ^{13}C-NMR: 165.3 (*s*); 155.1 (*s*); 148.5 (*s*); 148.2 (*s*); 137.9 (*d*); 128.9 (*s*, C(5,9)); 121.6 (*d*); 120.0 (*d*); 116.2 (*d*); 110.3 (*d*); 110.0 (*d*); 56.0 (*q*). HR-EI-MS: 259.0725 ($[M-H]^+$; $C_{13}H_{11}N_2O_4^+$; calc. 259.0719).

DISCOtech Pharmacophore Generation. Pharmacophore modeling studies were performed using the SYBYL 8.1 suit of programs (*Tripos Discovery Informatics*, St. Louis, Missouri) installed on a *DELL* desktop workstation equipped with a dual 2.0 GHz *Intel*® *Xeon*® processor running the Red Hat Enterprise Linux (version 5) operating system. The chemical structures of hydantoin derivatives were sketched in SYBYL 8.1 and assigned *Gasteiger* partial charges, and energy minimized using Tripos Force Field to a final root-mean-square gradient of 0.01 kcal/mol to obtain the local minimum. Diverse conformations of each compound were generated using stochastic conformational analysis tool in SYBYL. The DISCOtech module on SYBYL 8.1 was used to build pharmacophore models based on common chemical features. DISCOtech-generated initial pharmacophore features were edited to remove the receptor interaction sites like H-bond donor and acceptor sites present in the receptor. Overall alignment score and the associated pharmacophore features were analyzed for the selection of appropriate pharmacophore model.

DISCOtech Pharmacophore Model Scores. The score of individual pharmacophore model was calculated according to the following equation:

$$\text{Score} = \frac{H}{M} \sum_{\text{allfeat}} \frac{d_{ij} - d_0}{k/(k-1)} 10^{(k-0.5 \sum_{\text{alloverlaps}} ij)} \tag{1}$$

where: *H*, number of molecules that match the model; *M*, number of targets (molecules in the input set); *k*, number of features; d_{ij}, interface distance; d_0, 2 A^0; all feat, all features; all overlaps, all overlapping features.

All the features were calculated in the model, features that are closer to each other than 2 A^0 will attract a penalty, while features that are further apart than 2 A^0 will attract a positive score term. Penalty and bonus were involved in the scoring formula, which constitutes an important aspect in the scoring function. Penalty occurs for any mismatched molecules and for features closer than 2 A^0. Bonus occurs for features further than 2 A^0 and for features further than tolerance. However, there was a lack of bonus (not a penalty) for features closer than tolerance.

Drug-Likeness Score Predictions. The compounds' overall potential to qualify for a drug can be determined by the combination of factors such as drug-likeness, cLog*P*, log*S*, molecular weight, and toxicity risks [54][55]. This value was calculated by multiplying individual properties using the following equation:

$$ds = \pi\left(\frac{1}{2} + \frac{1}{2}s_i\right) \cdot \pi \cdot t_i \tag{2}$$

where *ds* is the drug score, s_i are the contributions calculated directly from cLog*P*, log*S*, molecular weight, and drug-likeness (p_i) *via Eqn. 3* describing a spline curve. Parameters *a* and *b* are (1, −5), (1, 5), (0.012, −6) and (1, 0) for cLog*P*, log*S*, molecular weight, and drug-likeness, resp. [54][55]. t_i are the

contributions taken from four toxicity risk types. The t_i values of 1.0, 0.8, and 0.6 stand for no risk, medium risk, and high risk, resp.

$$s = \frac{1}{1 + e^{ap+b}} \tag{3}$$

Wound-Healing Assay. Prostate adenocarcinoma (human) cell line (PC-3) were maintained in *RPMI-1640* supplemented with 2 mmol/l glutamine, 10% fetal bovine serum (FBS), 100 μg/ml penicillin G, and 100 μg/ml streptomycin [34–36]. Briefly, the cells were allowed to grow to 100% confluency in 24-well plates. Once a monolayer developed, the same area of each well was then displaced by scratching a line through the layer and a wound made with a sterile 100 μl pipette tip. The detached/floating cells were then washed two times with PBS and finally with serum-free medium (SFM). The cells were then re-fed with fresh medium *RPMI-1640* containing 0.5% FBS and were treated with or without each of the tested compounds for a period of 24 h. The cells were then fixed, stained with *Diff-Quick*™ (*Dade Behring*, Newark, DE) and measurements of the wound area were photographed digitally with an inverted microscope [34–40]. The total number of cells migrated was calculated for each condition. All experiments were conducted independently in triplicate.

REFERENCES

[1] A. Jemal, R. Siegel, E. Ward, Y. Hao, J. Xu, M. J. Thun, *CA Cancer J. Clin.* **2009**, *59*, 225.
[2] American Cancer Society, http://www.cancer.org, accessed on March 9, 2010.
[3] J. Jongsma, M. H. Oomen, M. A. Noordzij, W. M. Van Weerden, G. J. M. Martens, T. H. van der Kwast, F. H. Schröder, G. J. van Steenbrugge, *Prostate* **2002**, *50*, 203.
[4] Y. Furuya, K. Akakura, S. Akimoto, H. Inomiya, H. Ito, *Int. J. Urol.* **1999**, *6*, 240.
[5] N. Segawa, I. Mori, H. Utsunomiya, M. Nakamura, Y. Nakamura, L. Shan, K. Kakudo, Y. Katsuoka, *Pathol. Int.* **2001**, *51*, 452.
[6] M. Mudit, M. Khanfar, A. Muralidharan, S. Thomas, G. V. Shah, R. W. M. van Soest, K. A. El Sayed, *Bioorg. Med. Chem.* **2009**, *17*, 1731.
[7] G. V. Shah, A. Muralidharan, S. Thomas, M. Gokulgandhi, M. Mudit, M. Khanfar, K. El Sayed, *Mol. Cancer Ther.* **2009**, *8*, 509.
[8] G. L. Patrick, 'An Introduction to Medicinal Chemistry', 3rd edn., Oxford University Press Inc., New York, 2005.
[9] K. R. Acharya, E. D. Sturrock, J. K. Riodan, M. R. W. Ehlers, *Nat. Rev. Drug Discovery* **2003**, *2*, 891.
[10] A. A. Patchett, E. Harris, E. W. Tristram, M. J. Wyvratt, M. T. Wu, D. Taub, E. R. Peterson, T. J. Ikeler, J. ten Broeke, L. G. Payne, D. L. Ondeyka, E. D. Thorsett, W. J. Greenlee, N. S. Lohr, R. D. Hoffsommer, H. Joshua, W. V. Ruyle, J. W. Rothrock, S. D. Aster, A. L. Maycock, F. M. Robinson, R. Hirschmann, C. S. Sweet, E. H. Ulm, D. M. Gross, T. C. Vassil, C. A. Stone, *Nature* **1980**, *288*, 280.
[11] D. J. Abraham, 'Burger's Medicinal Chemistry and Drug Discovery', 6th edn., John Wiley and Sons, New York, 2003.
[12] A. P. Feinberg, I. Creese, S. H. Snyder, *Proc. Natl. Acad. Sci. U.S.A.* **1976**, *73*, 4215.
[13] C. R. Ganelllin, S. M. Roberts, 'Medicinal Chemistry – The Role of Organic Chemistry in Drug Research', 2nd edn., Academic press, New York, 1994.
[14] R. B. Silverman, 'The Organic Chemistry of Drug Design and Drug Action', 2nd edn., Elsevier Academic Press, MA, 2004.
[15] B. W. Richardson, *Med. Times Gaz.* **1869**, *2*, 703.
[16] A. B. H. Funcke, M. J. E. Ernsting, R. F. Rekker, W. T. Nauta, *Arzneim. Forsch.* **1953**, *3*, 503.
[17] A. K. Ghose, J. J. Wendoloski, *Persp. Drug Discovery Design* **1998**, *9–11*, 253.
[18] G.-Z. Ao, Y.-H. Zhang, H. Ji, G. Deng, *Yaoxue Xuebao* **2004**, *39*, 803.
[19] C. Syldatk, V. Lehmensiek, G. Ulrichs, U. Bilitewski, K. Krohn, H. Höke, F. Wagner, *Biotechnol. Lett.* **1992**, *14*, 99.
[20] Y. Luo, L. Ma, H. Zheng, L. Chen, R. Li, C. He, S. Yang, X. Ye, Z. Chen, Z. Li, Y. Gao, J. Han, G. He, L. Yang, Y. Wei, *J. Med. Chem.* **2010**, *53*, 273.

[21] A. I. Khodair, A. A. El-Barbary, Y. A. Abbas, D. R. Imam, *Phosphorus, Sulfur Silicon Relat. Elem.* **2001**, *170*, 261.
[22] P. Kitipichai, R. La Peruta, G. M. Korenowski, G. E. Wnek, *J. Polym. Sci., Part A: Polym. Chem.* **1993**, *31*, 1365.
[23] A. K. Sen, S. Mukhopadhyay, *Indian J. Chem., Sect. B* **1983**, *22*, 939.
[24] B. Malhotra, A. K. Dwivedi, V. Hora, I. M. Hora, *J. Indian Chem. Soc.* **1990**, *67*, 74.
[25] J. Tanaka, K. Nakayasu, Patent FR 2585701 A1, 1987.
[26] K. R. Bharucha, V. Pavilanis, D. Ajdukovic, H. M. Schrenk, Patent DE 2329745, 1974.
[27] G. Billek, *Monatsh. Chem.* **1961**, *92*, 352.
[28] W. A. Cetenko, D. T. Connor, R. J. Sorenson, P. C. Unangst, S. R. Stabler, Patent EP 343643, 1989.
[29] S. Ostergaard, H. B. Olsen, N. C. Kaarsholm, P. Madsen, P. Jakobsen, S. Ludvigsen, G. Schluckebier, D. B. Steensgaard, A. K. Petersen, Patent WO 2004080480, 2004.
[30] M. Lamiri, K. Bougrin, B. Daou, M. Soufiaoui, E. Nicolas, E. Giralt, *Synth. Commun.* **2006**, *36*, 1575.
[31] L. Weiss, *Cancer Metastasis Rev.* **2000**, *19*, 193.
[32] I. J. Fidler, *Nat. Rev. Cancer* **2003**, *3*, 453.
[33] M. G. Lampugnani, *Methods Mol. Biol.* **1999**, *96*, 177.
[34] K. V. Lu, K. A. Jong, A. K. Rajasekaran, T. F. Cloughesy, P. S. Mischel, *Lab. Investig.* **2004**, *84*, 8.
[35] B. Herren, K. J. Garton, S. Coats, D. F. Bowen-Pope, R. Ross, E. W. Raines, *Exp. Cell Res.* **2001**, *271*, 152.
[36] C. Huang, Z. Rajfur, C. Borchers, M. D. Schaller, K. Jacobson, *Nature* **2003**, *424*, 219.
[37] K. T. Mc Henry, S. V. Ankala, A. K. Ghosh, G. Fenteany, *ChemBioChem* **2002**, *3*, 1105.
[38] A. Vogt, K. E. Pestell, B. W. Day, J. S. Lazo, P. Wipf, *Mol. Cancer Ther.* **2002**, *1*, 885.
[39] C. Klein-Soyer, J. P. Cazenave, J. M. Herbert, J. P. Maffrand, *J. Cell Physiol.* **1994**, *160*, 316.
[40] E. G. Fischer, A. Stingl, C. J. Kirkpatrick, *J. Immunol. Methods* **1990**, *128*, 235.
[41] D. Philp, T. Huff, Y. S. Gho, E. Hannappel, H. K. Kleinman, *FASEB J.* **2003** *17*, 2103.
[42] E.-J. Moon, Y. M. Lee, O.-H. Lee, M.-J. Lee, S.-K. Lee, M.-H. Chung, Y.-I. Park, C.-K. Sung, J.-S. Choi, K.-W. Kim, *Angiogenesis* **1999**, *3*, 117.
[43] P. C. Ma, T. Kijima, G. Maulik, E. A. Fox, M. Sattler, J. D. Griffin, B. E. Johnson, R. Salgia, *Cancer Res.* **2003**, *63*, 6272.
[44] R. S. Chung, P. A. Adlard, J. Dittmann, J. C. Vickers, M. I. Chuah, A. K. West, *J. Neurochem.* **2004**, *88*, 454.
[45] L. W. Morgan, A. Wieslander, M. Davies, T. Horiuchi, Y. Ohta, M. J. Beavis, K. J. Craig, J. D. Williams, N. Topley, *Kidney Int.* **2003**, *64*, 1854.
[46] Y. Saga, H. Mizukami, Y. Takei, K. Ozawa, M. Suzuki, *Int. J. Oncol.* **2003**, *23*, 1109.
[47] Y. C. Martin, M. G. Bures, E. A. Danaher, J. DeLazzer, I. Lico, P. A. Pavlik, *J. Comput.-Aided Mol. Des.* **1993**, *7*, 83.
[48] R. D. Clark, *J. Chem. Inf. Comput. Sci.* **1997**, *37*, 1181.
[49] D. P. Marriott, I. G. Dougall, P. Meghani, Y.-J. Liu, D. R. Flower, *J. Med. Chem.* **1999**, *42*, 3210.
[50] G. Spadoni, C. Balsamini, G. Diamantini, B. Di Giacomo, G. Tarzia, M. Mor, P. V. Plazzi, S. Rivara, V. Lucini, R. Nonno, M. Pannacci, F. Fraschini, B. M. Stankov, *J. Med. Chem.* **1997**, *40*, 1990.
[51] H.-J. Kim, H. Choo, Y. S. Cho, K. T. I. No, A. N. Pae, *Bioorg. Med. Chem.* **2008**, *16*, 636.
[52] D. S. Patel, P. V. Bharatam, *J. Comput.-Aided Mol. Des.* **2006**, *20*, 55.
[53] M. Khanfar, B. A. Asal, M. Mudit, A. Kaddoumi, K. A. El Sayed, *Bioorg. Med. Chem.* **2009**, *17*, 6032.
[54] I. V. Tetko, *Drug Discovery Today* **2005**, *10*, 1497.
[55] G. Szileighl, *Arzneim.-Forsch.* **1984**, *35*, 1260.

Received June 18, 2010